Efficient Resonant Loudspeakers with Large Form-Factor Design Freedom*

RONALD M. AARTS, *AES Fellow,* **JORIS A. M. NIEUWENDIJK, AND OKKE OUWELTJES**
(ronald.m.aarts@philips.com) (joris.nieuwendijk@chello.nl) (Okke.Ouweltjes@philips.com)

Philips Research Laboratories, 5656AE Eindhoven, The Netherlands

Small cabinet loudspeakers with a flat response are quite inefficient. Assuming that the frequency response can be manipulated electronically, systems that have a nonflat sound-pressure level (SPL) response can provide greater usable efficiency. Such a nonflat design can deal with very compact housing, but for small drivers it would require a relatively large cone excursion to obtain a high SPL. A new solution is presented that uses a resonant combination of a coupling volume and a long pipe-shaped port. In this structure the efficient resonant coupling of the driver to the acoustic load enables small drivers with modest cone displacement to achieve a high SPL. Due to the high and narrow peak in the frequency response, the normal operating range of the driver decreases considerably. This makes the driver unsuitable for normal use. To overcome this, a second measure is applied. Nonlinear processing essentially compresses the bandwidth of a 20–120-Hz 2.5-octave bass signal down to a much narrower span, which is centered where the driver efficiency is maximum. This system allows very compact loudspeakers. An experimental example of such a design is described, and a working prototype is discussed. The new loudspeaker is compared with a closed cabinet and a bass-reflex cabinet using the same drivers. It appears that the new loudspeaker has the highest output in its working range.

0 INTRODUCTION

There has been a longstanding interest in obtaining a high sound output from compact loudspeaker arrangements. The introduction of concepts such as flat TV and 5.1-channel sound reproduction systems has led to a renewed interest in obtaining a high sound output from compact loudspeaker arrangements with high efficiency. Compact relates here to both the volume of the cabinet into which the loudspeaker is mounted and the cone area of the loudspeaker. In conventional loudspeaker system design, the force factor *Bl* is chosen in relation to enclosure volume, suspension stiffness, cone diameter, and moving mass to yield a flat response over a specified frequency range. For small cabinet loudspeakers such a design is in general quite inefficient. It is not possible to combine a very high efficiency and a high sensitivity in a wide frequency range with a compact arrangement. On the other hand, assuming that the frequency response can be manipulated electronically, it then turns out that systems having a nonflat sound-pressure level (SPL) can provide greater usable efficiency, at least over a limited frequency range [1]–[3]. Such a design can deal with very compact housing, but for small drivers it requires a large cone displacement to obtain a high SPL. However, in this paper a new solution is presented, which uses a resonant combination of a coupling volume and a long pipe-shaped port. The efficient resonant coupling of the driver to the acoustic load in this structure enables small drivers with modest cone displacement to achieve a high SPL.

In the past much effort has been devoted to higher order band-pass systems using ports (see, for example, [4]–[6]). However, focus in that work was on designing systems with a reasonably broad bandwidth, while we are aiming for the highest efficiency, which implies a very small bandwidth, and hence a high quality factor of the system. We discuss these special resonant loudspeakers, which have a high SPL but require only a very low cone displacement. The dependence of the behavior of the transducer and its housing on various parameters, in particular the force factor *Bl* and the box and pipe dimensions, is investigated. For these special loudspeakers a practically relevant optimality criterion is defined. The desired characteristics are obtained at the expense of a decreased sound quality and the requirement of some additional electronics. It is discussed how such a special loudspeaker can

*Presented at the 120th Convention of the Audio Engineering Society, Paris, France, 2006 (May 20–23; revised 2006 August 21 and 30.

be made. It appears to be very cost-efficient and low-weight, and it has a high degree of freedom in the form-factor design of its cabinet. An example of such a design is described, and the performance of a working prototype is presented.

1 SPECIAL RESONANT LOUDSPEAKERS WITH HIGH QUALITY FACTOR *Q*

There exist well-known loudspeaker systems called "acoustic labyrinth loudspeakers" (from [7], cited in [8]—see Figs. 1 and 2—and [9], for other examples and historical notes see also [10], [11] for the corner ribbon loudspeaker). In such constructions the driver is mounted in a relatively long duct with a length approximately equal to one quarter of the wavelength corresponding to the open-air resonance frequency of the driver. However, those systems did not aim for a high quality factor Q. Olney wanted to lower the Q from curve A into curve B of the SPL response (Fig. 2, right panel). It has also been known for a long time, that a misalignment of the parameters of vented boxes may result in a response with a high-Q peak (see for example, [12]).

The essential feature of the present work is that we are aiming for a high Q response of the system, rather than seeing this as a misalignment. We do this by using a system with a relatively long pipe, as shown schematically in Fig. 3. A specified frequency f_{work} nearly coincides with the Helmholtz or anti-resonance frequency, shown as f_b in Fig. 4. This f_{work} is the frequency (or a very narrow band) to which the low-frequency content of the signal is transferred, conforming to the mapping principle introduced in [2], and which is further discussed in Section 2. The frequency f_b is the frequency where the electrical input impedance curve reaches a local minimum between the first two impedance peaks; see Fig. 4. This ported cabinet is in

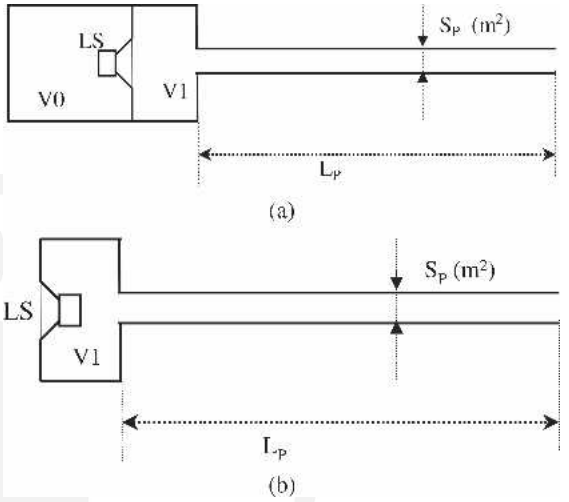

Fig. 3. Schematic construction of loudspeaker. (a) Band-pass enclosure with long port. (b) Bass-reflex enclosure with long port.

Fig. 1. Olney's acoustic labyrinth loudspeaker [7].

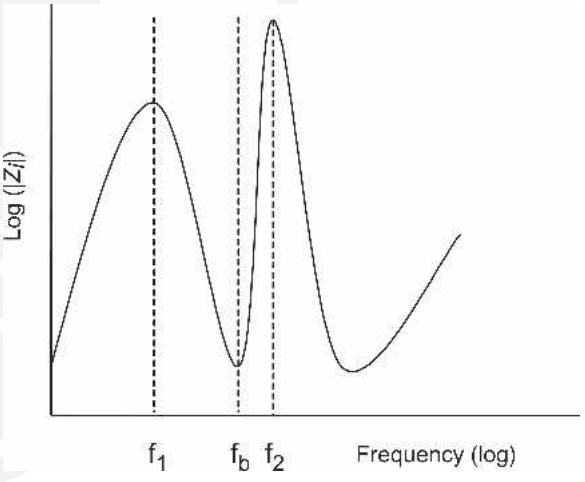

Fig. 4. Impedance of driver mounted in a pipe.

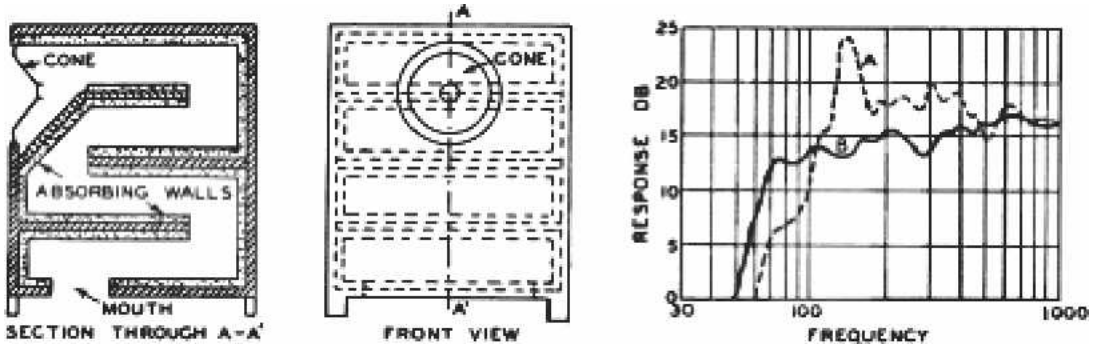

Fig. 2. Acoustic labyrinth loudspeaker from Olson [8].

contrast to [2]. There we used the fundamental resonance frequency of the system determined by the closed volume of the enclosure and the driver, while the modes of the enclosure were outside the frequency region of interest. Both systems have in common that a high-Q system is utilized. This makes the loudspeaker unsuitable for normal use. To overcome this, a second measure is applied. Nonlinear processing essentially compresses the bandwidth of a 20–120-Hz 2.5-octave bass signal down to a much narrower span, which is centered where the system efficiency is maximum. In the following we will discuss first the acoustical aspects of the system and then, in Section 2, the processing required.

We define the frequency f_0 for the configuration of Fig. 3(a) as the resonance frequency of the box with closed volume V_0 plus the driver, in the absence of volume V_1 and the pipe. In the case of Fig. 3(b) $f_0 = f_s$, where f_s is, as usual, the free air resonance frequency of the driver. With a band-pass box design, f_0 usually coincides with f_b. However, in our application f_0 can differ considerably from f_b.

The enclosure of Fig. 3(b) may look like a resonator, but the pipe is so long that it does not act like a Helmholtz resonator. This can be clarified by calculating the Helmholtz resonance frequency of a simple Helmholtz resonator, given as

$$f_H = \frac{c}{2\pi}\sqrt{\frac{S_p}{L_p' V_1}} \tag{1}$$

where L_p' is the effective pipe length, which will be discussed in Section 3. If the parameters of Table 1 are used in Eq. (1), then we get $f_H = 68$ Hz whereas the system has an antiresonance frequency of $f_b = 55$ Hz. Apparently the pipe is so long that we must use a transmission-line model, rather than applying Eq. (1). In the following we continue to denote the working frequency f_{work} by f_b, which applies for any length of pipe, in contrast to f_H, which together with Eq. (1) applies only to a system using a short pipe. We refer to a long pipe, somewhat arbitrarily, if $L_p > \lambda/10$, where $\lambda = c/f$ is the wavelength of the signal at the working frequency f. Mounting the pipe to a front volume V_1 has the advantages that the pipe length can be traded for the front volume without affecting efficiency at resonance, and that the driver diameter may be of a larger size than the pipe diameter, as shown schematically in Fig. 3.

Fig. 5 given the impedances and velocities occurring in the system's pipe of cross-sectional area S_p and length L_p. The band-pass system is modeled by the lumped-element model according to Fig. 6, with the loudspeaker elements given in Table 2 and the pipe element in Table 1. Furthermore the total spring constant of the driver suspension and the back volume V_0 (if there is any) is given by

$$k^* = C_{ms}^{-1} + \frac{\rho_0 c_0^2 S_1^2}{V_0} \tag{2}$$

where ρ_0 is the density and c_0 the speed of sound of the medium, and $C_1 = V_1 / (\rho_0 c_0^2 S_1^2)$ is the mechanical compliance of the front volume V_1. It is the combination of this front volume, the long pipe-shaped port, and the driver itself that enables an efficient resonant coupling between the driver and the acoustic load. We will discuss in the following the acoustics of the long port, which form an integral part of the resonating system.

If the air is vibrating harmonically with a frequency corresponding to the wavenumber $k = \omega/c$ and velocity v_{p1}, then the input mechanical impedance Z_1 is given by [13]

$$Z_1 = \rho_0 c_0 S_p \frac{\frac{Z_2}{\rho_0 c_0 S_p}\cos kL_p + j \sin kL_p}{j\frac{Z_2}{\rho_0 c_0 S_p}\sin kL_p + \cos kL_p}. \tag{3}$$

The velocity at the end of the pipe is

$$v_{p2} = \frac{v_{p1}}{j\frac{Z_2}{\rho_0 c_0 S_p}\sin kL_p + \cos kL_p}. \tag{4}$$

Looking at Eq. (4), we see that at frequencies such that $Z_2 \ll \rho_0 c_0 S_p$ and $\sin kL_p \approx 1$, v_{p2} can be much larger than v_{p1}. For these frequencies we get a gain of

$$\frac{v_{p2}}{v_{p1}} \approx \frac{\rho_0 c_0 S_p}{jZ_2}. \tag{5}$$

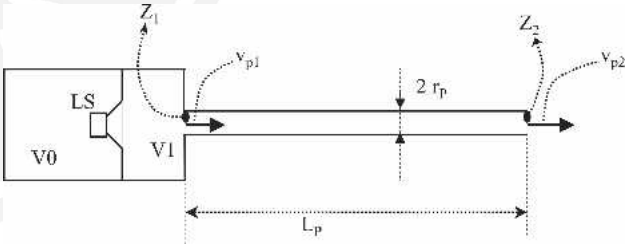

Fig. 5. Mechanical impedances Z_1, Z_2 and velocities v_{p1}, v_{p2} in system pipe.

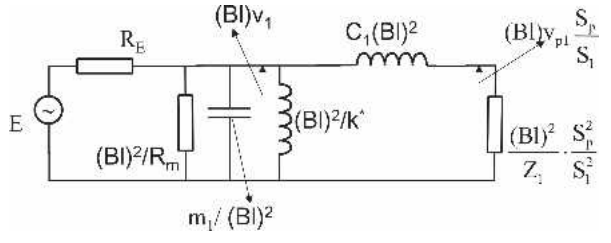

Fig. 6. Mobility-type lumped-element model of system according to Fig. 5. v_1—cone velocity; other parameters are given in Tables 1 and 2.

Table 1. Fitted parameters of prototype pipe.

Helmholtz frequency	f_b	55	(Hz)
Front volume	V_1	0.9	(l)
Port length	L_p	1.00	(m)
Efficient port length	L_p'	1.03	(m)
Port radius	r_p	0.0215	(m)
Port area	S_p	0.00145	(m^2)
Port losses	R_p	0.01575	(Ns/m)
Port losses	Q_p	30	(–)

It is this gain that we want to exploit. Usually in higher order band-pass systems one wants a certain bandwidth, but because we are interested in making a resonator, the bandwidth may be very small. The only limitation is the quality factor Q_p of the pipe, which is discussed in the Appendix. In order to optimize the SPL for a certain but fixed input power, we need to exploit the port resonance and optimize the force factor Bl for a given system geometry. We denote this particular optimal value of the force factor by Bl_o.

In the following we want to calculate the SPL of the system. Therefore we first need to calculate the acoustic power P_a delivered by the system. Using Eq. (3) to determine Z_1 from Z_2, Fig. 6 to determine the cone velocities v_1 and v_{p1}, and Eq. (4) to determine v_{p2} from v_{p1}, we can calculate the radiated acoustic power P_a at the pipe opening as

$$P_a = \frac{1}{2}|v_{p2}S_p|^2 R_{a\,rad} \tag{6}$$

where

$$R_{a\,rad} = \frac{\rho_0 \omega^2}{2\pi c_0} \tag{7}$$

is the approximated real part of the radiation impedance Z_2 in the low-frequency 2π field. Z_2 is defined as the usual mechanical radiation impedance plus an additional mechanical resistance due to pipe losses, yielding

$$Z_2 = R_p + jX_p \tag{8}$$

where R_p is the total mechanical resistance of the pipe, including the radiation resistance, seen as a lumped element at the end of the pipe, and X_p is the complex part of the mechanical radiation impedance at the end of the pipe. The preceding steps could be used to derive a single analytic expression for the SPL and the optimal Bl value. However, this would lead to a cumbersome formula, so we did the calculation numerically. By varying Bl we get the optimal value at the highest SPL. The relation between SPL at 1-m distance and η [2, eq. 32] is

$$\mathrm{SPL} = 112.18 + 10 \log \eta \tag{9}$$

where the system efficiency is

$$\eta(\omega) = \frac{P_a}{P_e} \tag{10}$$

and P_e is the electric power fed to the system, which for Eq. (9) and in the following we consider equal to 1 W (at $R_E = 2.8\ \Omega$ and $1.67\ V_{rms}$). Using Eqs. (6) and (9) we get the desired value for the SPL. The aim is to get the highest possible SPL, but this results in a narrow peak around f_{work} with a high Q. It appears—as for the closed-box system [2]—that if Bl is approximately equal to the optimal Bl, the highest peak in the SPL curve is reached and we have, for the electrical input impedance,

$$|Z_i|_{f=f_b, Bl=Bl_o} \approx 2R_E. \tag{11}$$

This relation appears to be very practical to see whether the optimal Bl_o has been chosen.

1.1 Resonant Band-Pass Loudspeaker

Fig. 7 displays the SPL in dB as a function of frequency (solid curve) for the system shown in Fig. 3(a), where m_1 has been increased to 24 g in order to obtain $f_0 = f_b = 55$ Hz, Bl has the theoretical optimal value of $Bl_o = 11.7$, and $V_0 = 2$ l. This value of Bl_o is rather high for such a small driver and is in contrast to [2]. There we used a closed volume, however. As a comparison the dashed curve in Fig. 7 shows the SPL of the same driver mounted in an infinite baffle with the same excursion as in the

Table 2. Parameters of prototype loudspeaker.

		I[a]	II[b]	III[c]	IV[d]	
Free-air resonance frequency	f_s	83.79	55.03	55.03	50.74	(Hz)
Mechanical quality factor	Q_{ms}	4.14	6.300	6.300	6.831	(–)
Electrical quality factor	Q_{es}	0.429	0.653	4.938	0.156	(–)
Total quality factor	Q_{ts}	0.389	0.592	2.768	0.153	(–)
Equivalent acoustic volume	V_{as}	0.365	0.365	0.365	0.365	(l)
Voice-coil dc resistance	R_E	2.80	2.80	2.80	2.80	(Ω)
Total moving mass	m_1	0.0088	0.0204	0.0204	0.024	(kg)
Mechanical compliance	C_{ms}	0.00041	0.00041	0.00041	0.00041	(m/N)
Mechanical resistance	R_m	1.12	1.12	1.12	1.12	(Ns/m)
Motor force factor	Bl	5.50	5.50	2.00	11.7	(N/A)
Membrane area	S_1	0.0025	0.0025	0.0025	0.0025	(m^2)
Reference efficiency	η	0.00049	0.000091	0.000012	0.000298	(%)
Produced sound pressure level	SPL	79.076	71.773	62.987	76.918	(dB)
Series lossless inductance	L_1	0.00044	0.00044	0.00044	0.00044	(H)
Mass	C_{mes}	0.00029	0.00067	0.0051	0.000175	(F)
Compliance	L_{ces}	0.0124	0.0124	0.00164	0.0561	(H)
Mechanical losses	R_{es}	27.01	27.01	3.57	122.22	(Ω)

[a] Nonmodified driver.
[b] Mass of driver increased to 20.4 g.
[c] Increased mass and lower Bl.
[d] Mass of driver increased to 24 g, optimal $Bl = 11.7$ N/A.

band-pass box. Fig. 7 clearly shows the extra gain in SPL obtained as the difference between the peaks and the dips of both curves at 55 Hz. Fig. 8 shows the corresponding electrical impedance of the system. The local minimum between the first peaks in Fig. 8 equals 5.6 Ω. This conforms to Eq. (11), $2R_{dc}$.

Fig. 9 gives the actual loudspeaker cone displacement. The maximum displacement reduction of the driver (see Fig. 9) coincides perfectly with the top of the SPL curve of Fig. 7.

1.2 Resonant Reflex Loudspeaker

Similar to the previous section, we will now study the reflex system of Fig. 3(b). Fig. 10 shows the SPL of a system according to Fig. 3(b). We see that at a work frequency $f_{work} = f_b$ the SPL is practically the same for the reflex system and the band-pass system because of the very low displacement of the loudspeaker. A deviation from the optimum value of Bl is not critical, provided that it is not too large.

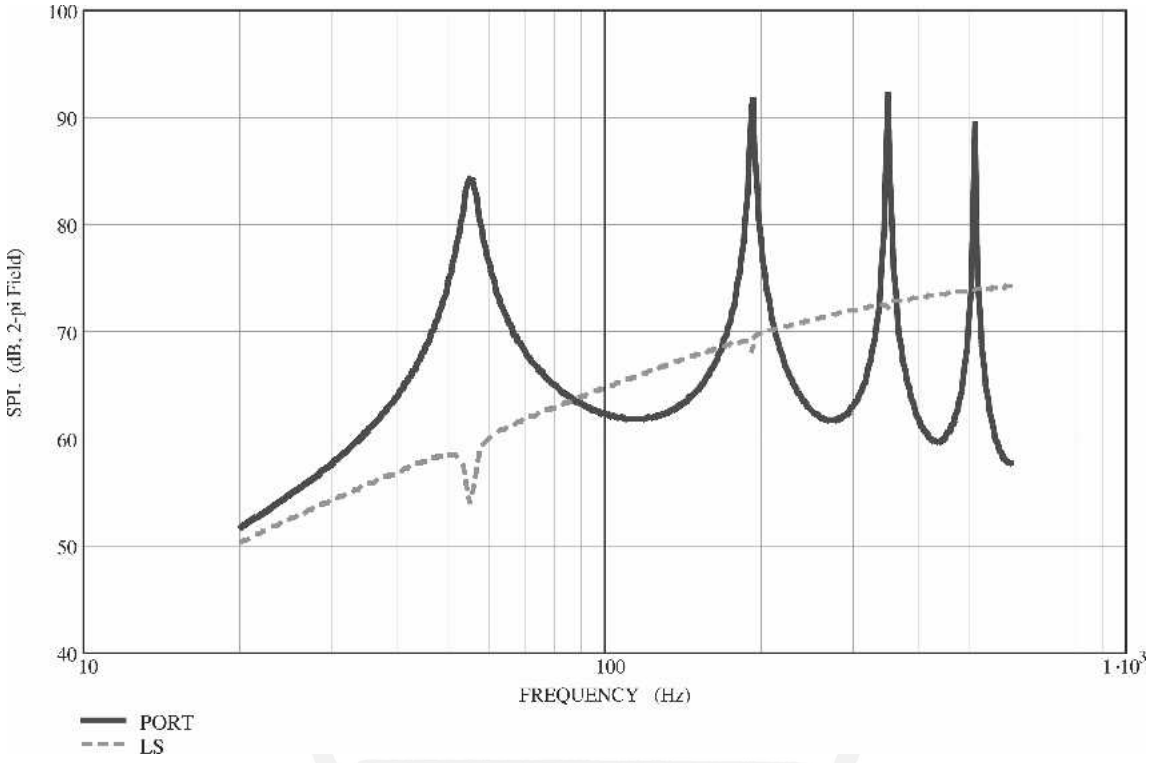

Fig. 7. SPL as a function of frequency for band-pass box of Fig. 3(a). ——— port only; - - - same loudspeaker in infinite baffle with same excursion as band-pass box. For parameters see Table 2, column IV, and Table 1.

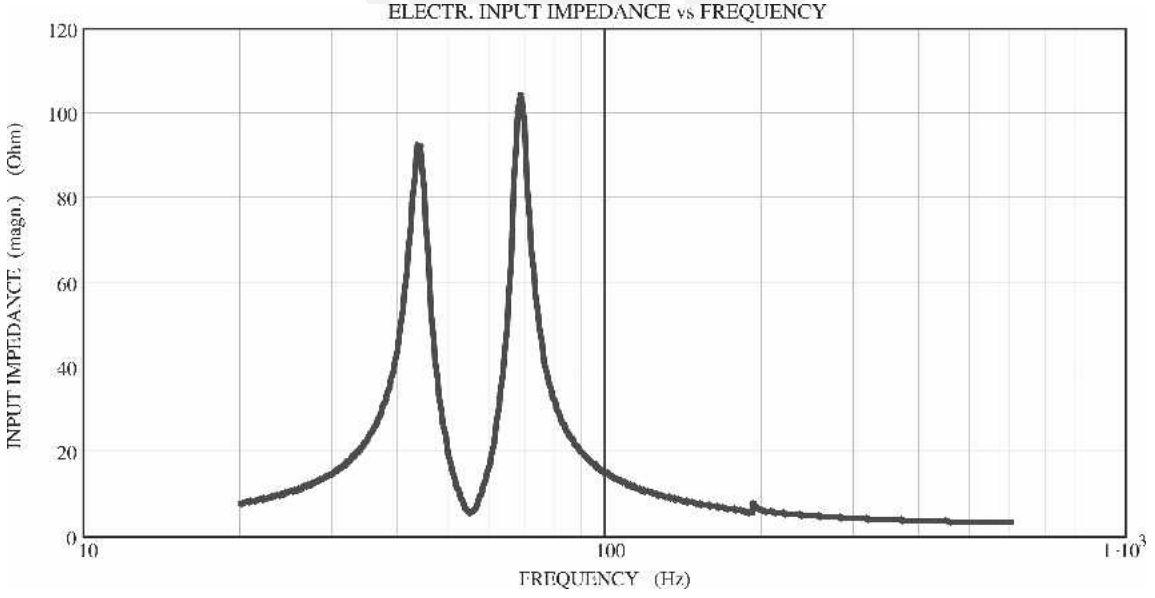

Fig. 8. Electrical input impedance (magnitude) as a function of frequency for band-pass box of Fig. 3(a). For parameters see Table 2, column IV, and Table 1.

Fig. 11 gives an example of a nonoptimal *Bl* value. In this case, with the same configuration as in Fig. 10, *Bl* has a value of 2, that is, a factor of 0.17 of the optimal *Bl* value. It appears that the maximum output no longer coincides with f_{work} of 55 Hz. The reduction in cone displacement remains the same, but the frequency response changes considerably, producing much less output at f_b and requiring very high cone excursions at the new frequency of maximum output. Also, but not shown here, the input impedance $Z_i \neq 2R_E$.

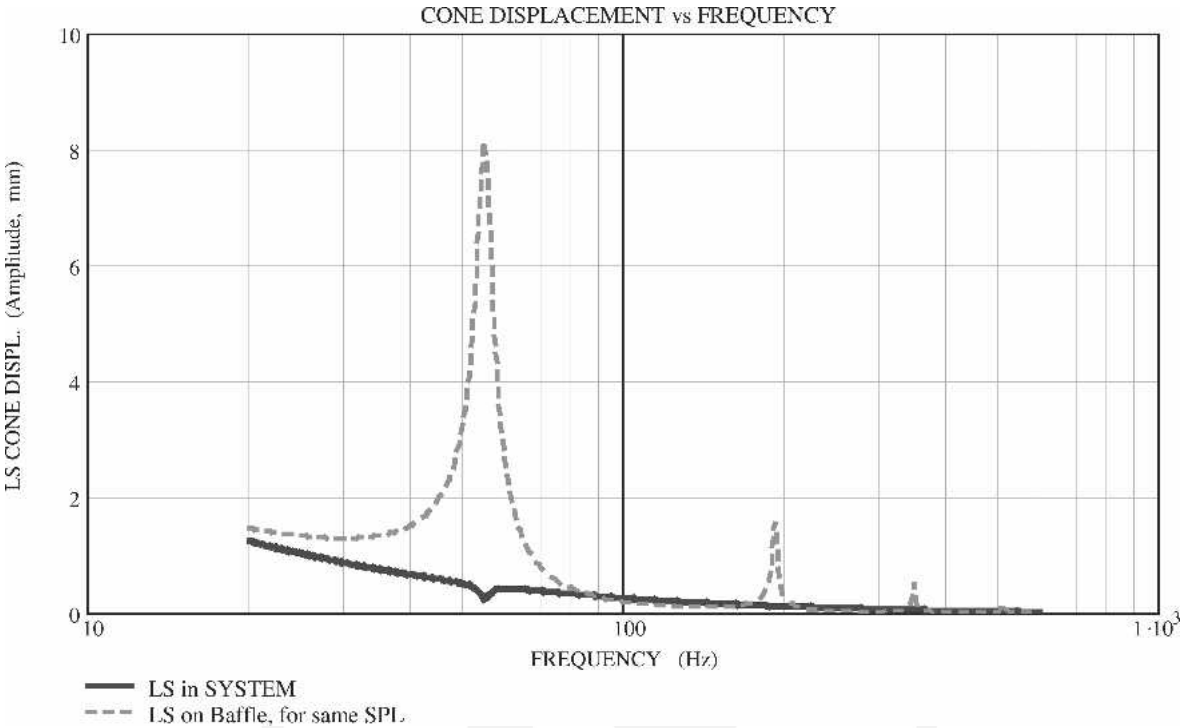

Fig. 9. Cone displacement as a function of frequency for band-pass box of Fig. 3(a). ——— loudspeaker in system; – – – same loudspeaker in infinite baffle with same SPL as band-pass box. For parameters see Table 2, column IV, and Table 1.

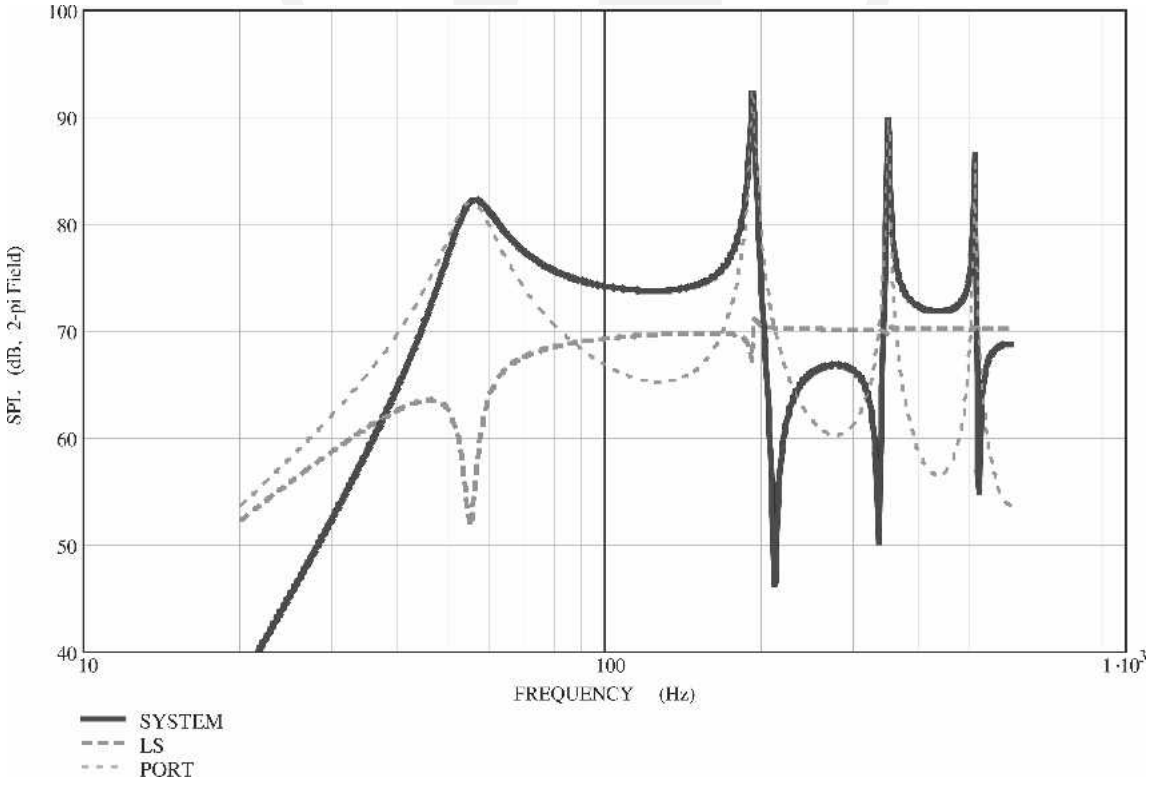

Fig. 10. SPL as a function of frequency for bass-reflex enclosure of Fig. 3(b). ——— system; - - - loudspeaker; – – – port only. For parameters see Table 2, column II, and Table 1.

Fig. 12 gives an example of the case where $f_b \neq f_0 = 84$ Hz, with a driver having $Bl = 5.5$, according to Table 2, column I.

Fig. 13 shows the corresponding electrical input impedance curve. Fig. 12 shows that, despite $f_b \neq f_0$, the SPL curve resembles the one of Fig. 10. The fact that f_b and f_0

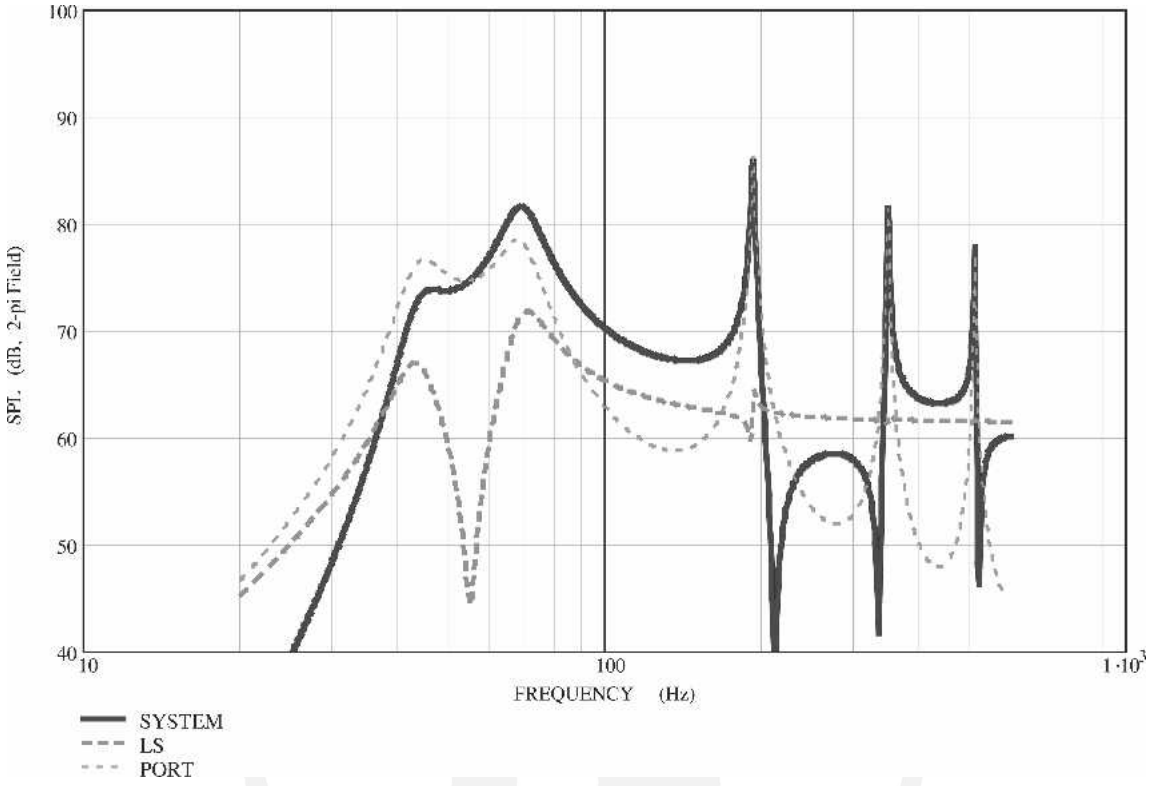

Fig. 11. SPL as a function of frequency for bass-reflex enclosure of Fig. 3(b) with nonoptimal *Bl* value. ——— system; - - - loudspeaker; – – – port only. For parameters see Table 2, column III, and Table 1.

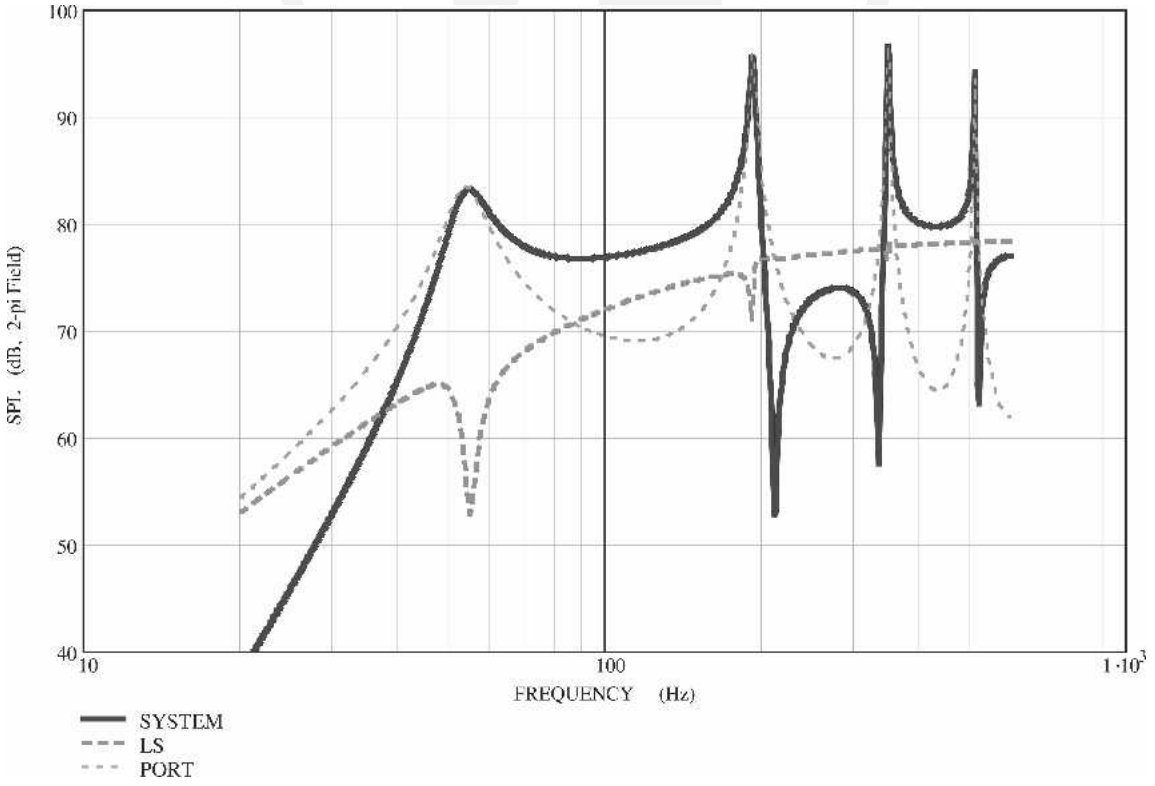

Fig. 12. SPL as a function of frequency for bass-reflex enclosure of Fig. 3(b), where $f_0 \neq f_b$, $f_0 = f_s = 84$ Hz. ——— system; - - - loudspeaker, – – – port only. For parameters see Table 2, column I, and Table 1.

do not necessarily need to be equal gives more design freedom. A practical consequence, for example, is that if $f_0 > f_b$, then the moving mass does not need to be increased to lower f_0.

To demonstrate the large form-factor design freedom, one of the prototypes is shown in two different views in Fig. 14, which is a folded version of Fig. 3(b). The loudspeakers are mounted on top. We used two loudspeakers because a single one with the desired cone area and *Bl* was not available. However, we consider those two as a single driver. Of course, other forms may be applied, such as bending the pipe around the screen of a flat TV set.

2 FREQUENCY MAPPING

Because of the typical high and narrow peaks in the frequency response (see Fig. 7) the useful operating range of the driver decreases considerably. This makes the driver unsuitable for normal use. To overcome this, a second measure is applied. Nonlinear processing essentially compresses the bandwidth of a 20–120-Hz 2.5-octave bass signal down to a much narrower span, which is centered at the SPL peak of the system. This can be done with a setup as depicted in Fig. 15 and will be discussed in the following.

The band-pass filter takes the band of interest, typically 20–120 Hz, and the envelope detector determines the envelope $m(t)$ of this signal. Then $m(t)$ is multiplied by a sinusoid of fixed amplitude and fixed frequency f_{work}. The result is that the coarse structure $m(t)$ (the envelope) of the music signal after the compression or "mapping" is the same as before the mapping; an example is shown in Fig. 16. But the fine structure has been changed to a sinusoid of fixed frequency f_{work}, which coincides with the peak in the SPL response. Fig. 16(a) shows the waveform of the bass content of a rock-music excerpt; the thin curve depicts its envelope $m(t)$. Fig. 16(b) and (c) gives the spectrograms of the input and output signals, respectively, clearly showing that the frequency bandwidth of the signal around 60 Hz decreases after the mapping, yet the temporal modulations remain the same [3].

3 EXPERIMENTAL RESULTS

The frequency response and the electrical input impedance of the system shown in Fig. 14 were measured. The measured impedance was used to determine the driver and pipe parameters, which are listed in Table 2, column I, and Table 1. The open end of the pipe, the drivers, and the microphone were at the corners of an equilateral triangle with sides of 1 m. The frequency response of the system when driven with 1-W power is shown in Fig. 17 (solid curve). The frequency response was computed as well.

Fig. 14. Experimental setup. "Pipe" is folded four times. Opening in front of cylinder is "end of pipe." Cavity between the drivers and grey upper disc is volume V_1 and is connected to "pipe" via circle segment.

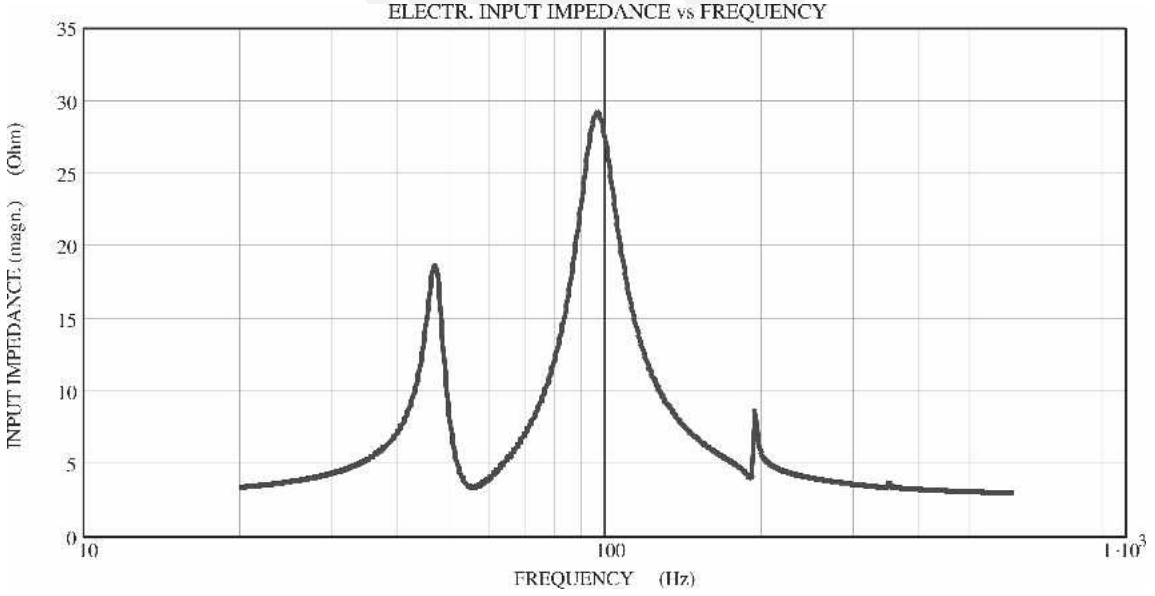

Fig. 13. Electrical input impedance (magnitude) as a function of frequency corresponding to Fig. 12, where $f_0 \neq f_b, f_0 = f_s = 84$ Hz. For parameters see Table 2, column I, and Table 1.

The pipe length L_p and the Q_p of the model parameters were chosen such that they resemble the measurement. The computed result is plotted as the dashed curve in Fig. 17. The corresponding measured and calculated electrical input impedances of the system are shown in Fig. 18. It appears that the computed result matches the measured result quite well. This is for the parameters L_p and Q_p chosen sensibly, as discussed hereafter. The physical length L_p of the pipe is equal to 1 m. Due to the complex radiation impedance of the pipe, it seems that the pipe is longer. This is known as the end correction [13],

$$L_p' = L_p + 0.6r_p. \tag{12}$$

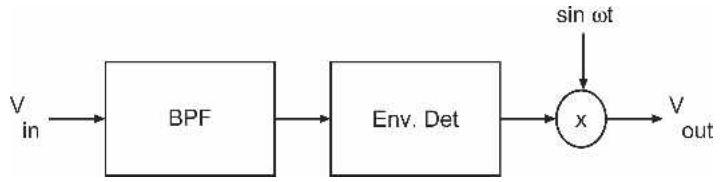

Fig. 15. Setup of mapping scheme. BPF—band-pass filter; Env. Det.—envelope detector. Signal V_{out} is fed to power amplifier and finally to driver.

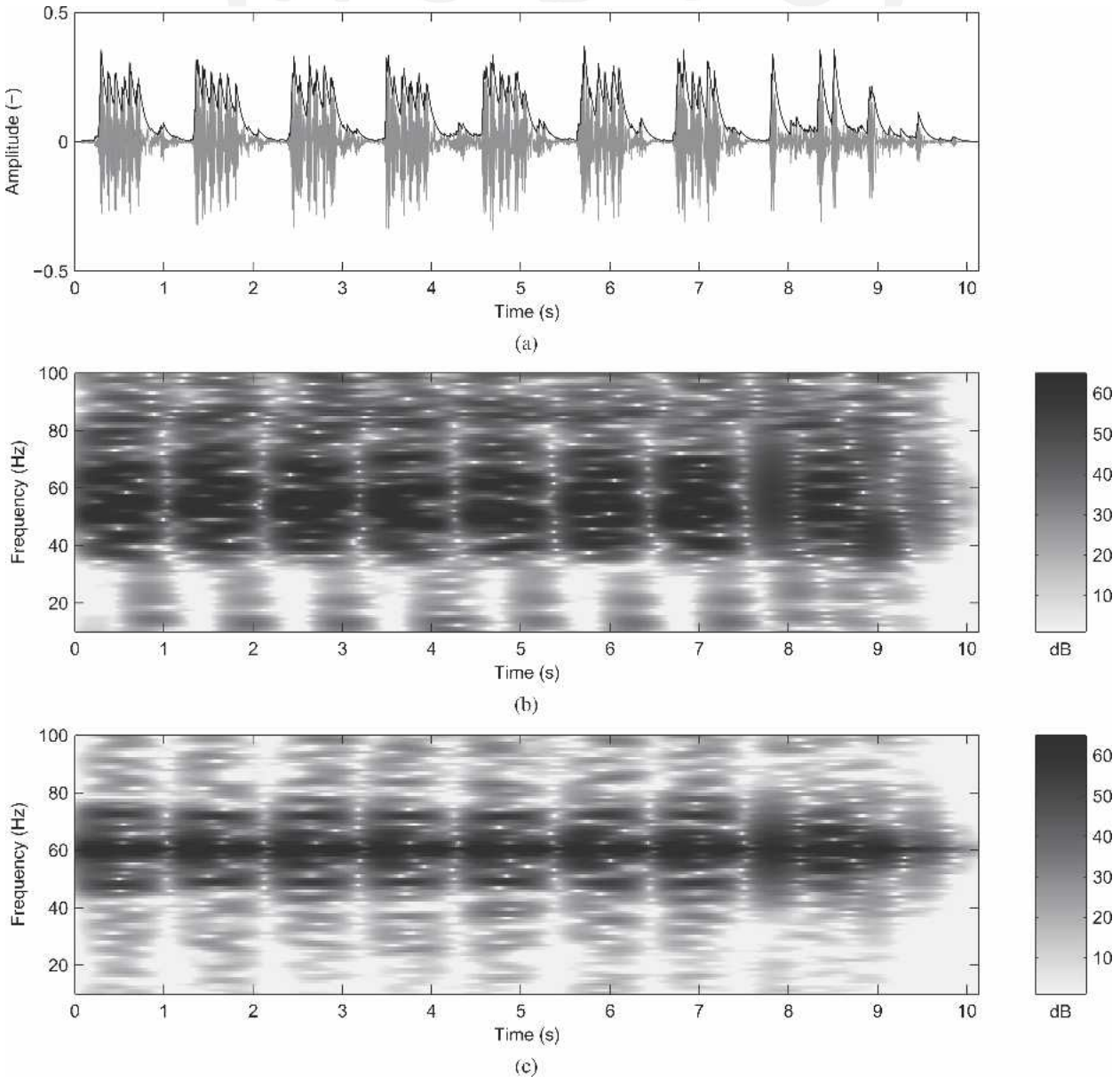

Fig. 16. Signals before and after frequency-mapping processing of Fig. 15. (a) Time signal at V_{in}. —— output of envelope detector. (b), (c) spectrograms of input and output signals.

When the port losses $R_p = 0.01575$ N·s/m are introduced into the calculation, we get a good resemblance to the measured data. We consider R_p here as a total (including the radiation losses) lumped mechanical-impedance parameter at the end of the port, that is, R_p is equal to the real part of Z_2 (see Fig. 5), while for the radiation computations

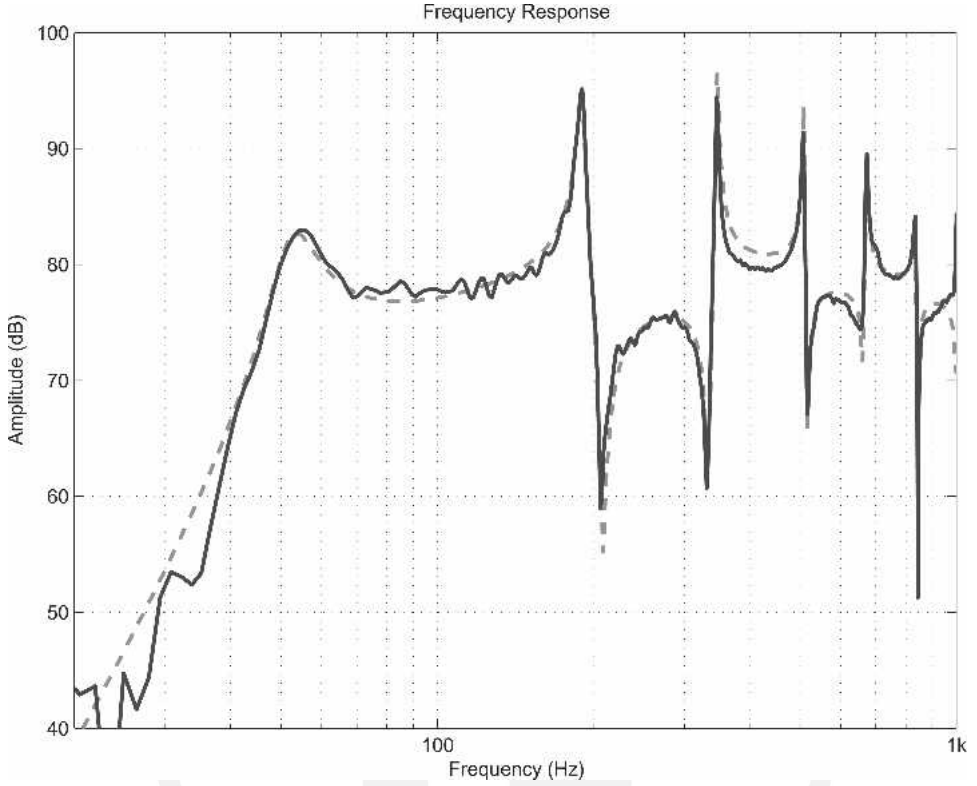

Fig. 17. Measured (——) and calculated (– – –) frequency responses of system of Fig. 14. Port damping in calculations was $R_p = 0.01575$ N·s/m. For parameters see Table 2, column I, and Table 1.

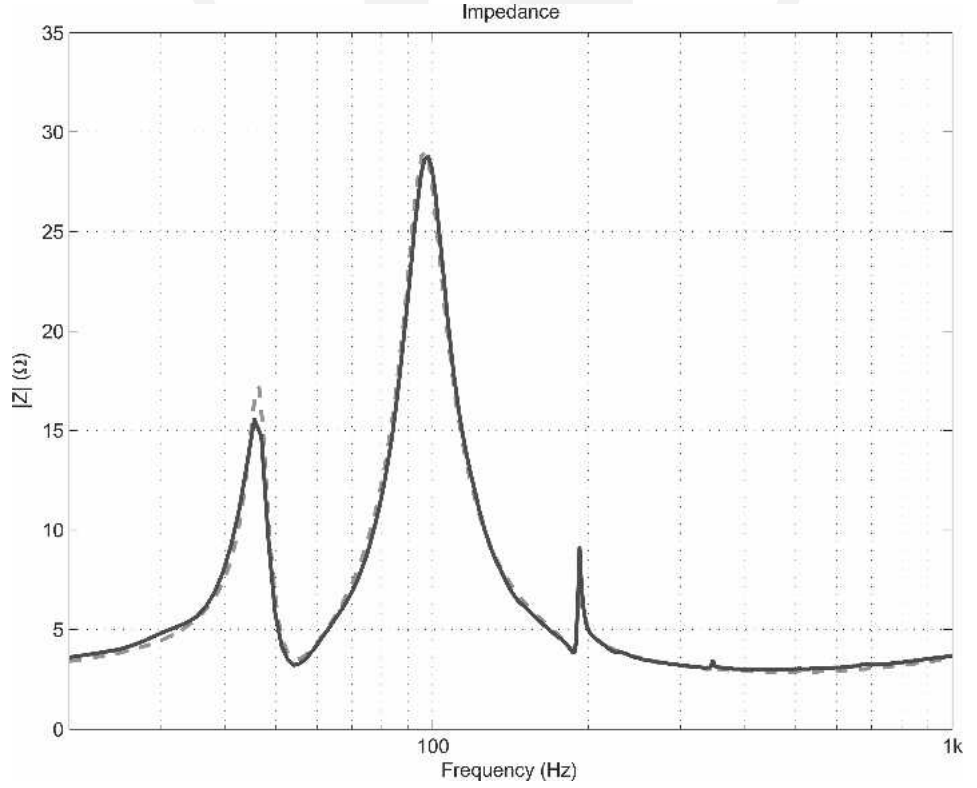

Fig. 18. Measured (——) and calculated (– – –) electrical impedances of system of Fig. 14. Port damping in calculations was $R_p = 0.01575$ N·s/m. For parameters see Table 2, column I, and Table 1.

we use Eqs. (6) and (7). To demonstrate this effect, if we neglect the port losses, we obtain the curves in Figs. 19 and 20, corresponding to Figs. 17 and 18, respectively. This shows that the peak in the SPL around 55 Hz could have been a little higher. It appears also that the other peaks at higher frequencies become much higher.

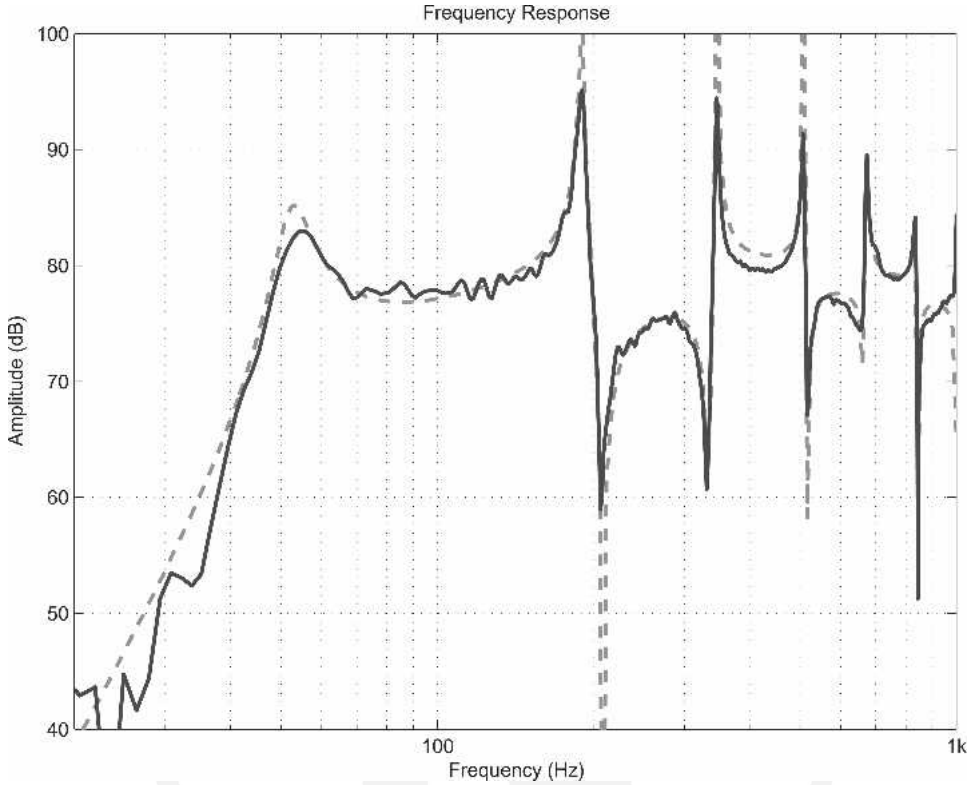

Fig. 19. Measured (——) and calculated (– – –) frequency responses of system of Fig. 14. Port damping was practically neglected in calculations. For parameters see Table 2, column I, and Table 1.

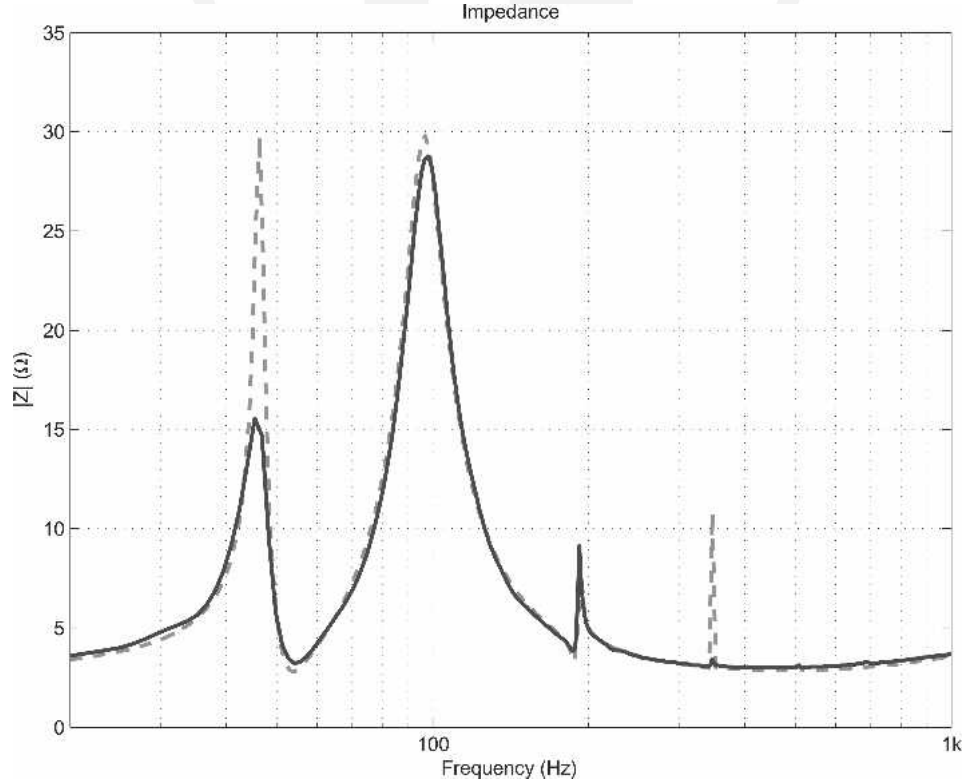

Fig. 20. Measured (——) and calculated (– – –) electrical impedances of system of Fig. 14. Port damping was practically neglected in calculations. For parameters see Table 2, column I, and Table 1.

4 DISCUSSION

An old loudspeaker designer's dilemma is "do we want high efficiency or small enclosure?" This dilemma is partially solved by using the high-Q band-pass box concept, as discussed, but at the expense of decreased sound quality and the need for some additional electronics to accomplish the frequency mapping. While the new loudspeaker is not a HiFi one, many informal listening tests and demonstrations[1] confirmed that the decrease in sound quality appears to be modest, apparently because the auditory system is less sensitive at low frequencies. Also, the other parts of the audio spectrum have a distracting influence on this mapping effect, which has been confirmed during formal listening tests [14], where the detectability of mistuned fundamental frequencies was determined for a variety of realistic complex signals. Finally, the part of the spectrum that is affected is only between, say, 20 and 120 Hz, so the higher harmonics of these low notes are mostly out of this band and are thus not affected. They will contribute to the missing fundamental effect in their normal unprocessed fashion. All these factors support the notion that detuning becomes difficult to detect once the target complex is embedded in a spectrally and temporally rich sound context, as is typical for applications in modern multimedia reproduction devices [14].

Finally, Fig. 21 compares the SPL of this new loudspeaker with a classic closed cabinet (thin dashed curve), a quasi Butterworth third-order (QB3) bass-reflex alignment (heavy dashed curve), and the new loudspeaker (solid curve). The QB3 is the most commonly used vented alignment because it yields a smaller cabinet volume for a given driver. The volume of the closed box and that of the new loudspeaker, including its long pipe, are both 2.4 l. The volume of the bass-reflex cabinet is dictated by the driver parameters and the QB3 alignment and has a total volume of 1.6 l, its port radius and length are 11 mm and 0.60 m, respectively, and $f_H = 38$ Hz. In all three cases the same drivers are used, as listed in Table 2, columm II. In Fig. 22 the corresponding displacement curves are plotted. It appears that the new loudspeaker has the highest output in its working range of 55 Hz, whereas the closed cabinet is very inefficient and the QB3 alignment is in between. The QB3 alignment has a lower cutoff frequency than the new loudspeaker, but this range is also covered by the new loudspeaker because of the mapping technique described in Section 2. The corresponding displacement curves of Fig. 22 clearly show that the new loudspeaker has the lowest cone displacement in its working range.

5 CONCLUSIONS

In a small cabinet it is not possible to obtain both high efficiency and high sensitivity in a wide frequency range. The force factor *Bl,* enclosure, and port design play a very important role in loudspeaker design. They determine efficiency, sensitivity, impedance, SPL response, weight, and cost. It appears that the optimal *Bl* value for the new system must be rather high.

A new loudspeaker has been developed which, together with some additional electronics, yields a large form-factor design freedom. In addition it can be a compact, sensitive, and relatively efficient loudspeaker system, re-

[1]Demonstrations are on http://www.dse.nl/~rmaarts.

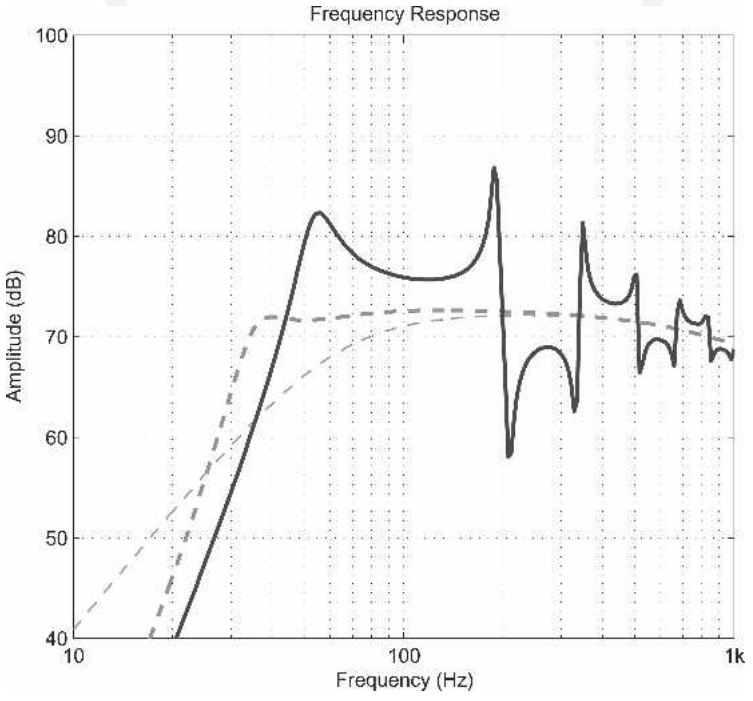

Fig. 21. Comparison of the SPIs of three different loudspeakers with the same drivers (at 1 W in R_E, 1 m, 2π field). – – – closed cabinet; ▬ ▬ QB3 bass-reflex alignment; ▬▬ new loudspeaker as shown in Fig. 3(b). For driver parameters see Table 2, column II; for long-port cabinet see Table 1.

quiring a relatively low cone excursion, which makes the system very suitable for low-frequency sound reproduction.

6 REFERENCES

[1] E. Larsen and R. M. Aarts, *Audio Bandwidth Extension. Application of Psychoacoustics, Signal Processing and Loudspeaker Design* (Wiley, New York, 2004).

[2] R. M. Aarts, "High-Efficiency Low-*Bl* Loudspeakers," *J. Audio Eng. Soc.,* vol. 53, pp. 579–592 (2005 July/Aug.).

[3] R. M. Aarts, "Optimally Sensitive and Efficient Compact Loudspeakers," *J. Acoust. Soc. Am.,* vol. 119, pp. 890–896 (2006 Feb.).

[4] L. R. Fincham, "A Bandpass Loudspeaker Enclosure," presented at the 63rd Convention of the Audio Engineering Society, *J. Audio Eng. Soc. (Abstracts),* vol. 27, p. 600 (1979 July/Aug.), preprint 1512.

[5] E. R. Geddes, "An Introduction to Band-Pass Loudspeaker Systems," *J. Audio Eng. Soc.,* vol. 37, pp. 308–342 (1989 May).

[6] J. A. M. Nieuwendijk, "Band-Pass Loudspeaker Enclosure with Long Port," presented at the 94th Convention of the Audio Engineering Society, *J. Audio Eng. Soc. (Abstracts),* vol. 41, pp. 394, 396 (1993 May), preprint 3508.

[7] B. Olney, "A Method of Eliminating Cavity Resonance, Extending Low Frequency Response and Increasing Acoustic Damping in Cabinet Type Loudspeakers," *J. Acoust. Soc. Am.,* vol. 8, pp. 104–111 (1936).

[8] H. F. Olson, *Acoustical Engineering* (Van Nostrand, New York, 1957).

[9] P. Wilson and G. L. Wilson, "Horn Theory and the Phonograph," *J. Audio Eng. Soc.,* vol. 23, pp. 194–199 (1975 Apr.).

[10] http://www.quadesl.org/History/Quad_History/quad_history.html (2006 July).

[11] "Corner Ribbon Loudspeaker," *Wireless World,* p. 11 (1950 Jan.).

[12] R. H. Small, "Vented-Box Loudspeaker Systems, Part I: Small-Signal Analysis," *J. Audio Eng. Soc.,* vol. 21, pp. 363–372 (1973 June).

[13] L. E. Kinsler, A. R. Frey, A. B. Coppens, and J. V. Sanders, *Fundamentals of Acoustics* (Wiley, New York, 1982).

[14] N. Le Goff, R. M. Aarts, and A. G. Kohlrausch, "Thresholds for Hearing Mistuning of the Fundamental Component in a Complex Sound," in *Proc. 18th Int. Cong. on Acoustics (ICA2004),* (Kyoto, Japan, 2004), p. I-865, paper Mo.P3.21.

[15] M. J. Moloney and D. L. Hatten, "Acoustic Quality Factor and Energy Losses in Cylindrical Pipes," *Am. J. Phys.,* vol. 69, pp. 311–314 (2001 Mar.).

APPENDIX
Acoustic quality factor of the port

The quality factor Q_p is defined [15] as

$$Q_p = \frac{\omega E_{tot}}{P_{tot}} \tag{13}$$

where P_{tot} is the total port power due to radiation, thermal, and viscous losses, and is related to the total (lumped) port losses R_p as

$$P_{tot} = \frac{1}{2}|v_{p2}|^2 R_p. \tag{14}$$

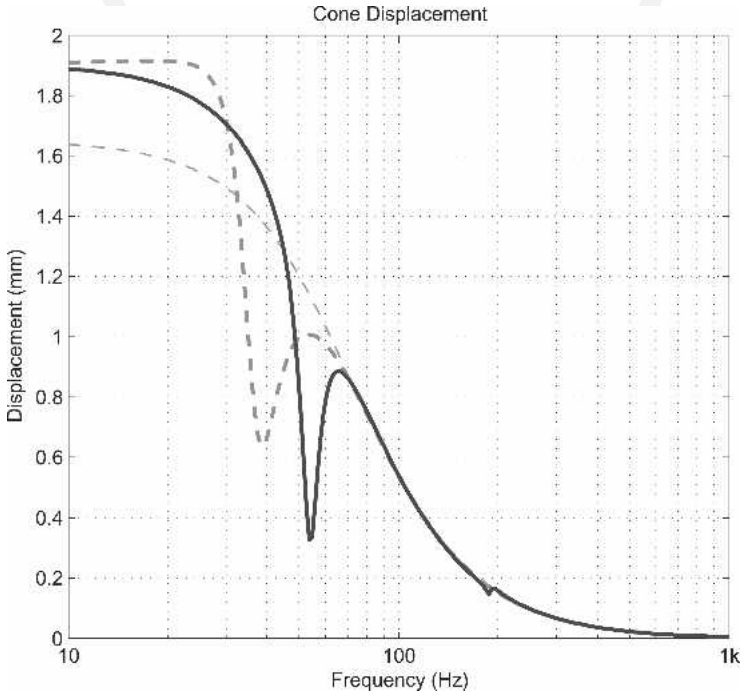

Fig. 22. Comparison of driver displacements in three different cabinets but with the same drivers (at 1 W in R_E). ▬ ▬ closed cabinet; – – – QB3 bass-reflex alignment; ▬▬ new loudspeaker as shown in Fig. 3(b). For driver parameters see Table 2, column II; for long-port cabinet see Table 1.

In simple harmonic motion, the total energy in a cylindrical pipe containing a standing sinusoidal wave with maximum velocity v_{p2} at one end may be written as the maximum kinetic energy that is equal to

$$E_{tot} = \frac{1}{4}\rho v_{p2}^2 S_p L_p. \tag{15}$$

Combining Eqs. (13)–(15) results in

$$Q_p = \frac{\omega \rho S_p L_p}{2R_p} \tag{16}$$

or for a pipe of length $L_p = \lambda/4 = c/4f$,

$$Q_p = \frac{\pi S_p \rho c}{4R_p}. \tag{17}$$

Eq. (17) is a convenient way to relate the total pipe losses R_p to the total Q_p of a quarter-lambda pipe. The Q due to the radiation (2π field) only is

$$Q_{rad} = \frac{cL_p}{2S_p f} \tag{18}$$

and for a baffled quarter-lambda pipe,

$$Q_{rad} = \frac{c^2}{8S_p f^2}. \tag{19}$$

For frequencies in the bass range we get, using Eq. (19), values for Q_{rad} which are more than ten times higher than the observed total Q_p, which is usually less than 50. Apparently the radiated acoustic power contributes only in a very small extent to the total damping ($R_{rad} \ll R_p$).

THE AUTHORS

R. M. Aarts

J. A. M. Nieuwendijk

O. Ouweltjes

Ronald M. Aarts was born in Amsterdam, The Netherlands, in 1956. He received a B.Sc. degree in electrical engineering in 1977, and a Ph.D. degree in physics from the Delft University of Technology, Delft, The Netherlands, in 1995.

He joined the optics group at Philips Research Laboratories, Eindhoven, The Netherlands, in 1977. There he initially investigated servos and signal processing for use in both Video Long Play players and Compact Disc players. In 1984 he joined the acoustics group and worked on the development of CAD tools and signal processing for loudspeaker systems. In 1994 he became a member of the digital signal processing (DSP) group and has led research projects on the improvement of sound reproduction by exploiting DSP and psychoacoustical phenomena. In 2003 he became a research fellow and extended his interests in engineering to medicine and biology.

Dr. Aarts has published a large number of papers and reports and holds over one hundred granted and pending U.S. patents in these fields. He has served on a number of organizing committees and as chair for various international conventions. He is a senior member of the IEEE, a fellow and governor of the AES, and a member of the NAG (Dutch Acoustical Society), the Acoustical Society of America, and the VvBBMT (Dutch Society for Biophysics and Biomedical Engineering). He is a part-time full professor at the Eindhoven University of Technology.

Joris A. M. Nieuwendijk was born in 's-Hertogenbosch, The Netherlands, in 1946. He studied physical engineering at the Technical University of Eindhoven, where he received an M.Sc. degree in 1971. He then joined one of the Philips Laboratories in Eindhoven and worked in the area of deflection coils for color tubes and high-resolution monochrome tubes. In 1979 he joined the acoustics group of the Advanced Project Laboratories of Philips Consumer Electronics and since then has worked on loudspeaker predevelopment.

Mr. Nieuwendijk holds a number of patents in this area. He is an active musician who plays the bass tuba.

●

Okke Ouweltjes was born in 's-Hertogenbosch, The Netherlands, in 1972. He received a B.Sc. degree in applied physics in 1997. As a software engineer he was involved in audio watermarking and audio fingerprinting. In 2002 he became a member of the DSP group of the Philips Research Laboratories in Eindhoven, where he is working on the improvement of low-frequency sound reproduction. His main interest is the combination of acoustics, loudspeakers, and signal processing.

Mr. Ouweltjes is a member of the AES and the NAG (Dutch Acoustical Society).